

Alexander Kuehne, Adrian Loch, Thomas Nitsche, Joerg Widmer, Matthias Hollick, and Anja Klein, "BER Enhancements for Practical Interference Alignment in the Frequency Domain," in *Proc. International Symposium on Wireless Communication Systems (ISWCS)*, August 2014.

©2008 IEEE. Personal use of this material is permitted. However, permission to reprint/republish this material for advertising or promotional purposes or for creating new collective works for resale or redistribution to servers or lists, or to reuse any copyrighted component of this works must be obtained from the IEEE.

# BER Enhancements for Practical Interference Alignment in the Frequency Domain

Alexander Kuehne\*, Adrian Loch<sup>†</sup>, Thomas Nitsche<sup>‡§</sup>, Joerg Widmer<sup>‡</sup>, Matthias Hollick<sup>†</sup>, and Anja Klein\*

\*Communications Engineering Lab, TU Darmstadt, Germany, {a.kuehne, a.klein}@nt.tu-darmstadt.de

<sup>†</sup>Secure Mobile Networking Lab, TU Darmstadt, Germany, {adrian.loch, matthias.hollick}@seemoo.tu-darmstadt.de

<sup>‡</sup>Institute IMDEA Networks, Madrid, Spain, {thomas.nitsche, joerg.widmer}@imdea.org

<sup>§</sup>Universidad Carlos III, Madrid, Spain

**Abstract**—The  $K$  user interference alignment scheme with symbol extensions proposed by Cadambe and Jafar achieves  $K/2$  degree of freedom in theory for high signal-to-noise ratios (SNRs). However, lower SNR ranges appear in many practical scenarios. Thus, further improvements of the Cadambe-Jafar scheme are demanded to enable interference alignment in more realistic settings. In this work, we propose a new precoding vector optimization that improves bit error rates (BER) using zero-forcing at the receivers. Furthermore, we compare and combine our approach with existing performance enhancement techniques for interference alignment such as orthonormalizing the precoding matrices or using lattice decoding instead of zero-forcing at the receiver. Finally, we implement interference alignment with symbol extension in the frequency domain along with the presented BER enhancement techniques on a software defined radio platform to validate our approaches. Both simulation results and testbed measurements show significant BER improvements for different  $M$ -QAM schemes compared to the original interference alignment mechanism. Moreover, our precoding optimization scheme based on zero-forcing outperforms lattice decoding in practical systems due to its lower sensitivity to real-world effects.

## I. INTRODUCTION

In [1], Cadambe and Jafar present a scheme for the  $K$  user frequency selective channel where each user can achieve  $K/2$  degrees of freedom (DoF) by using interference alignment (IA) at the transmitter and zero-forcing (ZF) at the receivers. IA is achieved by symbol extensions which can be applied in frequency using multiple subcarriers. The key idea behind IA is to align all interfering signals into a fraction of the signal space and using the remaining portion of the signal space to transmit the desired signals without interference. However, achieving promising gains in DoF using IA requires high signal-to-noise ratios (SNR). In practical systems with lower SNRs, the effective channel after interference alignment and removal applying ZF is strongly impaired, leading to high bit error rates (BER). Hence, techniques for improving the performance of the IA scheme of [1] for lower SNR ranges are essential. In the literature, there are two approaches to improve the performance. The first one is to optimize the precoding at the transmitter side. In [2], the authors show that by orthonormalizing the precoding matrices of [1] at the transmitter, the sum rate can be improved. In [3], the initial precoding vector  $\mathbf{w}$ , which is set to be the all-one vector in the original scheme of [1], is optimized to maximize the sum rate. The authors also show that it is possible to combine both

optimizing  $\mathbf{w}$  with orthonormalizing the precoding matrices, leading to further improvements. Both [2] and [3] consider the problem from a theoretical sum-rate-maximization perspective not taking into account the BER in practical settings. Another approach to improve the performance of IA is to apply a more sophisticated detector at the receiver. In [4], the use of lattice decoding (LD) instead of ZF is discussed for the IA scheme of [1]. Applying sphere decoding approaches, the BER improves significantly compared to conventional ZF. However, the authors neither consider the combination of LD with precoding vector optimization nor implement IA together with LD on a real testbed. The practical implementation of IA has recently drawn significant attention in the research community. [5] provides an overview of the practical challenges applying IA. However, current testbed implementations such as [6] and [7] mainly use spatial IA schemes based on [8] and [9], respectively, thus requiring multiple antennas. Furthermore, [10] and [11] present implementations of blind IA [12], which is another multiple antenna IA scheme that does not require any Channel State Information (CSI). In our previous work [13], we implemented frequency IA [1] applying ZF without any precoding optimization on a Software-Defined Radio (SDR). In this paper, we present the first practical implementation of frequency IA applying the afore mentioned BER enhancement techniques to further improve the performance. Our contributions are as follows:

- Proposal of a new precoding vector optimization tailored for BER enhancements applying frequency IA using ZF
- Combination and comparison of other BER enhancements for frequency IA applying ZF and LD
- Implementation of frequency IA along with the BER enhancement techniques on an SDR platform

The remainder of this paper is organized as follows. In Section II, we explain the system model and IA in the frequency domain. In Section III, we introduce three different BER enhancement techniques together with our newly proposed precoding vector optimization and we discuss possibilities for combining these techniques. In Section IV, we present simulation results and discuss testbed measurements. Finally, we conclude the paper in Section V.

## II. SYSTEM MODEL

In the following, we present the system model for the 3 user case, applying the frequency IA scheme of [1] with a

precoding block length of  $N_P = 2n + 1$  subcarriers with  $n \geq 1$ . We assume Orthogonal Frequency Division Multiple Access (OFDMA) with  $N = k \cdot N_P$  ( $k \in \mathbb{N}$ ) subcarriers. We form  $k$  groups of  $N_P$  subcarriers to build a precoding block by grouping the  $i$ -th subcarrier together with the  $(j \cdot k + i)$ -th subcarrier with  $j = 1, \dots, N_P - 1$  [13]. With this distributed resource allocation, the channels of the subcarriers within one precoding block can be assumed to be uncorrelated for channels with a corresponding coherence bandwidth such as typical indoor channels [13]. In the following, we consider one given precoding block.

Transmitter 1 encodes the  $(n + 1) \times 1$  vector  $\mathbf{x}_1$  with precoding matrix  $\mathbf{V}_1 \in \mathbb{C}^{(2n+1) \times (n+1)}$  while transmitter 2 and 3 encode the  $n \times 1$  vectors  $\mathbf{x}_2$  and  $\mathbf{x}_3$  with precoding matrices  $\mathbf{V}_2, \mathbf{V}_3 \in \mathbb{C}^{(2n+1) \times n}$ , respectively. The received signal  $\mathbf{r}_i$  at the  $i$ -th receiver can then be written as

$$\mathbf{r}_i = \mathbf{H}_{i1} \mathbf{V}_1 \mathbf{x}_1 + \mathbf{H}_{i2} \mathbf{V}_2 \mathbf{x}_2 + \mathbf{H}_{i3} \mathbf{V}_3 \mathbf{x}_3 + \mathbf{z}_i \quad (1)$$

where  $\mathbf{H}_{ij}$  is the channel matrix of size  $(2n + 1) \times (2n + 1)$  and  $\mathbf{H}_{ij} = \text{diag}(h_{ij}[1], h_{ij}[2], \dots, h_{ij}[2n + 1])$   $i, j = 1, 2, 3$ .  $h_{ij}[s]$  denotes the complex channel transfer function of the channel from transmitter  $i$  to receiver  $j$  on subcarrier  $s$ , with  $h_{ij}[s] \sim \mathcal{CN}(0, 1)$  and  $\mathbf{z}_i \sim \mathcal{CN}(0, \sigma_n^2)$  denoting the AWGN at receiver  $i$ . With the average SNR  $\bar{\gamma}$ , the noise variance is given by  $\sigma_n^2 = \frac{1}{\bar{\gamma}}$ , and we assume  $\sigma_n^2$  to be equal for all receivers.

The precoding matrices  $\mathbf{V}_i$  are designed in such a way that the interfering signals at the different receivers occupy a common signal space, i.e., the interference is aligned. This can be achieved using the following design similar to [1]:

$$\mathbf{V}_1 = \mathbf{T}_2 [\mathbf{T}_1^{-1} \mathbf{w} \quad \mathbf{w} \quad \mathbf{T}_1 \mathbf{w} \quad \dots \quad \mathbf{T}_1^{n-1} \mathbf{w}] \quad (2)$$

$$\mathbf{V}_2 = [\mathbf{w} \quad \mathbf{T}_1 \mathbf{w} \quad \mathbf{T}_1^2 \mathbf{w} \quad \dots \quad \mathbf{T}_1^{n-1} \mathbf{w}] \quad (3)$$

$$\mathbf{V}_3 = \mathbf{T}_3 [\mathbf{w} \quad \mathbf{T}_1 \mathbf{w} \quad \mathbf{T}_1^2 \mathbf{w} \quad \dots \quad \mathbf{T}_1^{n-1} \mathbf{w}] \quad (4)$$

with

$$\mathbf{T}_1 = (\mathbf{H}_{12})^{-1} \mathbf{H}_{13} (\mathbf{H}_{23})^{-1} \mathbf{H}_{21} (\mathbf{H}_{31})^{-1} \mathbf{H}_{32} \quad (5)$$

$$\mathbf{T}_2 = (\mathbf{H}_{31})^{-1} \mathbf{H}_{32} \quad (6)$$

$$\mathbf{T}_3 = (\mathbf{H}_{13})^{-1} \mathbf{H}_{12}. \quad (7)$$

The  $(2n + 1) \times 1$  vector  $\mathbf{w}$  can be chosen freely, e.g., the all-one vector as done in [1]. As long as vector  $\mathbf{w}$  has no zero entries, the  $\frac{3n+1}{2n+1}$  degrees of freedom can be achieved [2].

Before transmission, a power normalization of the precoding vectors is performed to guarantee that the total transmit power  $P_T$  of all three users over the  $N_P$  subcarriers is equal to  $N_P$ . This can be achieved by scaling  $\mathbf{w}$  with a power normalization factor as explained in Section III-A. Note that we do not assume a per-user power constraint but a total one, since with more relaxed power constraints also lattice decoding becomes possible (c.f. Section III-C).

At receiver  $i$ , the interference can be zero-forced using the  $(2n + 1) \times (2n + 1)$  ZF filter matrix  $\mathbf{A}_i = (\mathbf{B}_i)^{-1}$ , where the  $k$ -th column  $B_{i,k}$  of matrix  $\mathbf{B}_i$  is given by

$$B_{i,k} = \begin{cases} \mathbf{H}_{i1} \mathbf{V}_{1,k} & k = 1, \dots, n + 1 \\ \mathbf{H}_{i2} \mathbf{V}_{2,k-n-1} & k = n + 2, \dots, 2n + 1 \cup i = 1, 2 \\ \mathbf{H}_{i3} \mathbf{V}_{3,k-n-1} & k = n + 2, \dots, 2n + 1 \cup i = 3 \end{cases} \quad (8)$$

with  $\mathbf{V}_{i,k}$  denoting the  $k$ -th column of precoding matrix  $\mathbf{V}_i$ .

### III. BER ENHANCEMENT TECHNIQUES FOR IA IN THE FREQUENCY DOMAIN

In this section, we present three possible techniques to enhance the BER in comparison to the original IA scheme in [1] and we discuss the possibilities to combine these techniques.

#### A. Optimization of precoding vector

In [1], the initial precoding vector  $\mathbf{w}$  is arbitrarily set to be the all-one vector. This leaves room for further optimization. Kim and Torlak [3] propose a low complexity closed-form solution to maximize the lower bound to the sum rate. They show that this suboptimal solution performs close to the optimal global solution which has a much higher computational complexity. However, the authors perform the optimization using a sum rate criterion. For practical systems, the resulting BER is crucial. Hence, we propose to optimize  $\mathbf{w}$  such that the effective noise power after ZF is minimized for the different data streams at the corresponding receivers where a low effective noise translates to a low BER. To do so, we first derive the ZF matrix  $\mathbf{A}_i = (\mathbf{B}_i)^{-1}$  as a function of  $\mathbf{w}$ . Matrix  $\mathbf{B}_i$  can be written as  $\mathbf{B}_i = [\mathbf{b}_{i,1} \mathbf{w} \quad \mathbf{b}_{i,2} \mathbf{w} \quad \dots \quad \mathbf{b}_{i,2n+1} \mathbf{w}]$  with

$$\mathbf{b}_{i,k} = \begin{cases} \mathbf{H}_{i1} \mathbf{T}_2 \mathbf{T}_1^{k-2} & k = 1, \dots, n + 1 \\ \mathbf{H}_{i2} \mathbf{T}_1^{k-n-2} & k = n + 2, \dots, 2n + 1 \cup i = 1, 2 \\ \mathbf{H}_{i3} \mathbf{T}_3 \mathbf{T}_1^{k-n-2} & k = n + 2, \dots, 2n + 1 \cup i = 3 \end{cases} \quad (9)$$

as in (8). With the matrices  $\tilde{\mathbf{B}}_i = [\text{diag}(\mathbf{b}_{i,1}) \quad \dots \quad \text{diag}(\mathbf{b}_{i,2n+1})]$  and  $\tilde{\mathbf{C}}_i = (\tilde{\mathbf{B}}_i)^{-1}$ , which only depend on the channels between the users, the ZF matrix  $\mathbf{A}_i$  is given as

$$\mathbf{A}_i = \begin{bmatrix} \tilde{c}_{1,1}^{(i)} \frac{1}{w_1} & \dots & \tilde{c}_{1,2n+1}^{(i)} \frac{1}{w_{2n+1}} \\ \vdots & \ddots & \vdots \\ \tilde{c}_{2n+1,1}^{(i)} \frac{1}{w_1} & \dots & \tilde{c}_{2n+1,2n+1}^{(i)} \frac{1}{w_{2n+1}} \end{bmatrix} \quad (10)$$

with  $\tilde{c}_{j,k}^{(i)}$  denoting the  $j, k$ -th element of matrix  $\tilde{\mathbf{C}}_i$  and  $w_j$  denoting the  $j$ -th element of vector  $\mathbf{w}$ .

Next, we consider the power normalization mentioned in Section II. The total transmit power is given by

$$P_T = \left( \sum_{i=1}^3 \sum_{k=1}^n \mathbf{v}_{i,k}^H \mathbf{v}_{i,k} \right) + \mathbf{v}_{1,n+1}^H \mathbf{v}_{1,n+1} \quad (11)$$

assuming  $\mathbf{x}_i^H \mathbf{x}_i = 1$  for all  $i$  and superscript  $(\cdot)^H$  standing for complex conjugate transpose. Let  $\mathbf{G}$  denote a  $(2n + 1) \times (3n + 1)$  matrix whose  $i$ -th column  $\mathbf{G}_i$  is given by

$$\mathbf{G}_i = \begin{cases} \text{diag}(\mathbf{T}_2 \mathbf{T}_1^{i-2}) & i = 1, \dots, n + 1 \\ \text{diag}(\mathbf{T}_1^{i-n-2}) & i = n + 2, \dots, 2n + 1 \\ \text{diag}(\mathbf{T}_3 \mathbf{T}_1^{i-2n-2}) & i = 2n + 2, \dots, 3n + 1 \end{cases} \quad (12)$$

With  $g_i = \mathbf{G}_i^H \mathbf{G}_i$ , the total transmit power is given by  $P_T = \sum_{i=1}^{2n+1} g_i \cdot |w_i|^2$ . From this, it follows that vector  $\mathbf{w}$  needs to be scaled with normalization factor  $\sqrt{\frac{N_P}{P_T}}$ . Hence, the ZF

matrix including power normalization is given by

$$\mathbf{A}_{\text{norm},i} = \sqrt{\frac{P_T}{N_P}} \begin{bmatrix} \tilde{c}_{1,1}^{(i)} \frac{1}{w_1} & \cdots & \tilde{c}_{1,2n+1}^{(i)} \frac{1}{w_{2n+1}} \\ \vdots & \ddots & \vdots \\ \tilde{c}_{2n+1,1}^{(i)} \frac{1}{w_1} & \cdots & \tilde{c}_{2n+1,2n+1}^{(i)} \frac{1}{w_{2n+1}} \end{bmatrix}. \quad (13)$$

The goal is now to minimize the effective noise  $\tilde{\mathbf{z}}_i = \mathbf{A}_{\text{norm},i} \mathbf{z}_i$  after ZF at receiver  $i$ . Note that receiver 1 is only interested in the first  $n+1$  data symbols, while receiver 2 and 3 are interested in the last  $n$  data symbols. The noise variance  $\sigma_{i,j}^2$  of the effective noise experienced by the  $j$ -th data symbol at receiver  $i$  is given by

$$\sigma_{i,j}^2 = \frac{\sigma_n^2}{2n+1} \left( \sum_{k=1}^{2n+1} g_k \cdot |w_k|^2 \right) \cdot \left( \sum_{k=1}^{2n+1} \frac{|\tilde{c}_{j,k}^{(i)}|^2}{|w_k|^2} \right). \quad (14)$$

The objective function to be minimized is the sum of relevant effective noise powers at the corresponding receivers given by

$$P_n(\mathbf{w}) = \sum_{i=1}^3 \sum_{j \in \mathcal{S}(i)} \sigma_{i,j}^2 \quad (15)$$

with  $\mathcal{S}(1) = \{1, \dots, n+1\}$  and  $\mathcal{S}(l) = \{n+2, \dots, 2n+1\}$  for  $l = 2, 3$ . It can be rewritten as

$$P_n(\mathbf{w}) = \frac{\sigma_n^2}{2n+1} \left( \sum_{k=1}^{2n+1} g_k a_k + \sum_{k=1}^{2n+1} \sum_{\substack{j=1 \\ j \neq k}}^{2n+1} g_k a_j \frac{w_k^2}{w_j^2} \right) \quad (16)$$

with  $a_j = \sum_{i=1}^3 \sum_{l \in \mathcal{S}(i)} |\tilde{c}_{l,j}^{(i)}|^2$ . The optimized vector  $\mathbf{w}_{\text{opt}}$  is then found by solving the following optimization problem

$$\begin{aligned} \mathbf{w}_{\text{opt}} &= \arg \min_{\mathbf{w}} P_n(\mathbf{w}) \\ \text{s.t. } & w_j > 0 \quad j = 1, \dots, 2n+1. \end{aligned} \quad (17)$$

This kind of constrained nonlinear optimization problem can be solved applying, e.g., *fmincon* of MATLAB<sup>TM</sup> using also the gradient of  $P_n(\mathbf{w})$  with respect to  $w_j$  given by

$$P_{n,w_j}(\mathbf{w}) = \frac{2\sigma_n^2}{2n+1} \left( \sum_{\substack{k=1 \\ k \neq j}}^{2n+1} g_j a_k \frac{w_j}{w_k^2} - \sum_{\substack{k=1 \\ k \neq j}}^{2n+1} g_k a_j \frac{w_k^2}{w_j^3} \right) \quad (18)$$

Note that problem (17) is non-convex, i.e., it is not possible to guarantee that the global optimum can always be found. In the following, we refer to the optimization of the precoding vector as OPV.

### B. Orthonormalization of precoding matrices

In [2], the authors show that the maximum sum rate for a given precoding vector  $\mathbf{w}$ , e.g., the all-one vector, is achieved by orthonormalizing the precoding matrices  $\mathbf{V}_i$  of the different transmitters. This can be explained as follows. Calculating the precoding matrices  $\mathbf{V}_i$  determines the subspaces, i.e., the columns of  $\mathbf{V}_i$  such that the interference alignment conditions are fulfilled for a given  $\mathbf{w}$ . However, the arrangement of the precoding vector within each subspace can be chosen freely. From a signal-to-noise perspective, the best solution is to use orthogonal vectors since the signal power loss is minimized due to the orthogonal projection towards the

interfering signals using ZF. Hence, this technique can also be applied for reducing the BER. In the following, we refer to the orthonormalization of the precoding matrices as ONPM.

### C. Lattice decoding

In Section II, we showed how to detect the desired data streams at the corresponding receivers applying ZF. However, using ZF, the discrete nature of the interference is not taken into account, i.e., for receiver 1,  $\mathbf{x}_2$  and  $\mathbf{x}_3$  take values in  $\mathcal{C}^n$  assuming the symbols in  $\mathbf{x}_i$  are elements of a QAM signal constellation  $\mathcal{C}$  [4]. The idea is to perform a maximum likelihood detection by searching for the most likely transmitted symbols  $\mathbf{x}_j$  with  $j = 1, \dots, 3n+1$  given the received signal  $\mathbf{r}_i$  at receiver  $i$ . If the aligned interference signals not only lie in the same subspace, but also align at one discrete point, i.e.,  $\mathbf{H}_{12} \mathbf{V}_2 = \mathbf{H}_{13} \mathbf{V}_3$  for receiver 1, the so called lattice alignment is achieved [4]. Recalling (1), the signal at receiver 1 results in  $\mathbf{r}_1 = \mathbf{H}_{11} \mathbf{V}_1 \mathbf{x}_1 + \mathbf{H}_{12} \mathbf{V}_2 (\mathbf{x}_2 + \mathbf{x}_3) + \mathbf{z}_1$ . Hence,  $\mathbf{x}_{23} = \mathbf{x}_2 + \mathbf{x}_3$  takes values in  $\tilde{\mathcal{C}}^n$  with  $|\tilde{\mathcal{C}}| < |\mathcal{C}|^2$  where  $|\mathcal{C}|$  denotes the cardinality of  $\mathcal{C}$ , i.e., less constellation points need to be considered. For  $M$ -QAM, instead of considering  $M^{2n}$  possible constellation points for  $\mathbf{x}_2$  and  $\mathbf{x}_3$ , only  $(2\sqrt{M}-1)^{2n}$  possible constellation points for  $\mathbf{x}_{23}$  need to be considered. With  $\mathcal{Z}$  and  $\tilde{\mathcal{Z}}$  denoting finite subsets of integers from which constellations  $\mathcal{C}$  and  $\tilde{\mathcal{C}}$  are obtained by translation and scaling, the detector at receiver 1 can be written as

$$\hat{\mathbf{x}}_1 = \arg \min_{\mathbf{x}_1 \in \mathcal{Z}^{n+1}, \mathbf{x}_{23} \in \tilde{\mathcal{Z}}^n} \|\mathbf{r}_1 - \mathbf{H}_{11} \mathbf{V}_1 \mathbf{x}_1 - \mathbf{H}_{12} \mathbf{V}_2 \mathbf{x}_{23}\|^2 \quad (19)$$

This corresponds to decoding an integer lattice for which sphere decoding techniques can be applied, e.g., [14]. Similar derivations hold for receivers 2 and 3. Note that in order to fulfill lattice alignment, the precoding vectors  $\mathbf{V}_i$  calculated by (2) - (4) are not allowed to change after power normalization except for a scalar multiplication which must be identical for all users. Hence, a per-user power constraint as mentioned in Section II would violate the lattice alignment condition since the precoding vectors of different users would be scaled differently, i.e., a total power constrained normalization of the precoding vectors as shown in Section III-A needs to be done. In the following, we refer to lattice decoding as LD.

### D. Combination of techniques

Next, we discuss whether these BER enhancement techniques can be combined, and if so how this is done.

1) *OPV-ONPM-ZF*: As already mentioned in [3], OPV can be combined with ONPM using ZF. This is true for both the OPV scheme from [3] and our proposed OPV scheme. After determining  $\mathbf{w}_{\text{opt}}$ , the precoding matrices  $\mathbf{V}_i$  are computed according to (2) - (4). Afterwards, the columns of  $\mathbf{V}_i$  are orthonormalized. Combining OPV and ONPM leads to further BER enhancements as ONPM improves the BER for any given precoding vector  $\mathbf{w}$ —also for an optimally selected  $\mathbf{w}_{\text{opt}}$  whose corresponding precoding vectors are not necessarily mutually orthogonal in each subspace.

2) *OPV-LD*: Since the optimization of the precoding vector  $\mathbf{w}$  does not violate the lattice alignment condition, a combination of OPV with LD is feasible, leading to further BER enhancements compared to pure LD due to the optimized precoding vector  $\mathbf{w}_{\text{opt}}$ .

3) *ONPM-LD, OPV-ONPM-LD*: After the orthonormalization of the precoding matrices, the lattice alignment condition no longer holds, i.e., although the interference signals still lie in the same subspace, they no longer align at exact the same lattice point. Hence, using LD in combination with ONPM is not possible, i.e., also the combination OPV-ONPM-LD is not feasible.

#### IV. PERFORMANCE EVALUATION

##### A. Simulation results

In this section, we discuss the performance of the different BER enhancement schemes for the 3 user IA scheme assuming equal average SNR  $\bar{\gamma}$  for each user. For the evaluation, we assume perfect CSI at both the transmitters and the receivers, respectively. Fig. 1 depicts the BER averaged over all 3 receivers applying 4-QAM with  $n = 1$  as a function of the average SNR for all feasible combinations of BER enhancement schemes. The solid blue curves represent the IA schemes with  $\mathbf{w}$  the all-one vector applying pure ZF as done in [1], ZF with ONPM as done in [2] and pure LD as done in [4]. The dashed red curves are similar except that vector  $\mathbf{w}$  is optimized according to our proposal (OPV1), while vector  $\mathbf{w}$  of the dash-dotted green curves is optimized according to [3] (OPV2). The graphic highlights that all techniques outperform the original scheme of [1]. Moreover, applying only ZF at the receivers, we observe that our proposed combination OPV1-ONPM-ZF slightly outperforms OPV2-ONPM-ZF due to the fact that  $\mathbf{w}$  has been optimized to minimize noise power after ZF. Note that both OPV1-ONPM-ZF and OPV2-ONPM-ZF outperform pure LD although LD comes at much more complexity at the receiver compared to ZF. Applying LD at the receiver, the combination OPV2-LD using the  $\mathbf{w}$ -optimization of [3] outperforms OPV1-LD for high SNR. Obviously, maximizing sum rate is the better  $\mathbf{w}$ -optimization criterion to improve the maximum likelihood detection of LD compared to minimizing noise power after ZF although a significant improvement compared to pure LD can be seen also for OPV1-LD.

Fig. 2 shows the BER for 4-QAM, 16-QAM and 64-QAM with  $n = 1$ , where for each modulation scheme the BER of pure ZF, the optimized ZF (OPV1-ONPM-ZF) and the optimized LD (OPV2-LD) are depicted. Huge SNR gains can be achieved compared to the original IA scheme [1], e.g., at a BER of  $10^{-3}$ , applying 4-QAM with OPV1-ONPM-ZF, a

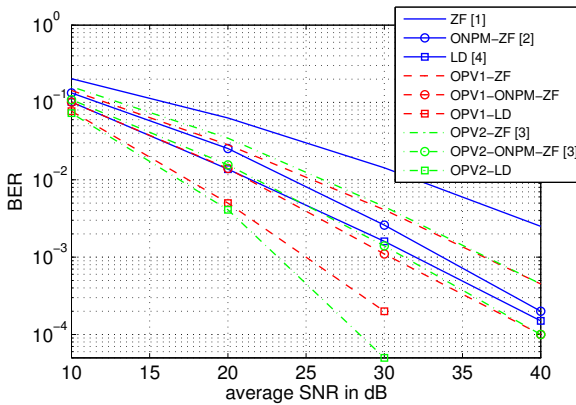


Fig. 1. BER vs. aver. SNR  $\bar{\gamma}$  for 4-QAM with  $n = 1$ .

gain of 17.5 dB can be achieved while applying OPV2-LD, a gain of 23 dB is possible. For higher modulation schemes, the gains are slightly smaller but still very large.

Fig. 3 depicts the same for the case  $n = 2$ . As shown in [4], increasing  $n$ , and thus, the DoF, leads to worse BER performances. It can be seen that the SNR gains in case of  $n = 2$  are even higher than in case of  $n = 1$ , due to the fact that the BER of the optimized ZF and LD schemes increases less severe compared to  $n = 1$  as the scheme of [1]. In practical scenarios with lower SNR ranges,  $n \leq 2$  is a good trade-off between BER and the number of transmitted data streams.

##### B. Testbed measurements

**Testbed.** We validate our simulative results on real-world channels using the reference design of SDR Wireless Open-Access Research Platform (WARP) [15]. Since our SDR has four radio interfaces, we place all three transmitters on one board and all three receivers on a second board. As a result, transmitters are automatically synchronized, similarly to access points connected via a wired backbone. While receivers are also synchronized, this is not needed for IA. We place senders and receivers along opposite walls of a rectangular lab room. The walls are separated 4.5 meters and within each group of transmitters/receivers, nodes are separated 1.3 meters. The resulting average SNR is about 30 dB.

**Experiment.** We measure the average BER over all receivers applying ZF, OPV2-LD and OPV1-ONPM-ZF since

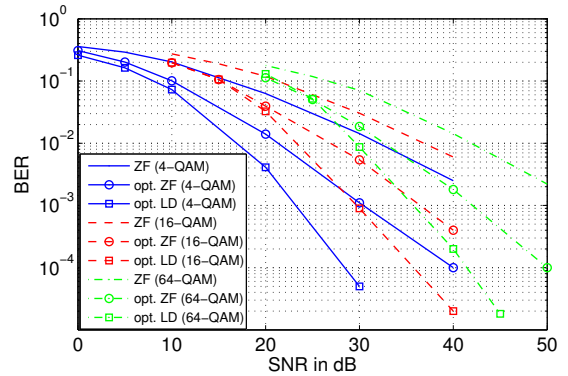


Fig. 2. BER vs. aver. SNR  $\bar{\gamma}$  for 4-QAM, 16-QAM and 64-QAM with  $n = 1$ .

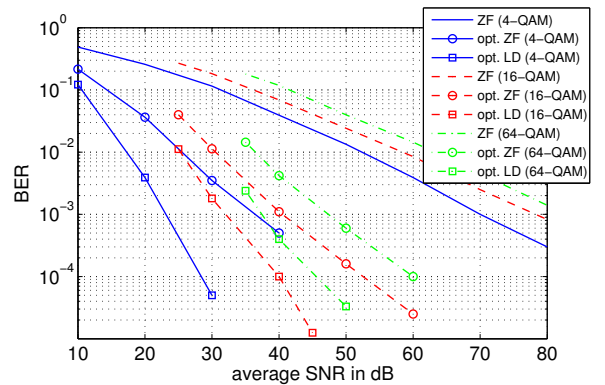


Fig. 3. BER vs. aver. SNR  $\bar{\gamma}$  for 4-QAM, 16-QAM and 64-QAM with  $n = 2$ .

their results are the most promising ones in the simulations. In each frame, transmitters send pilot symbols in a sequence to measure CSI. We assume an ideal CSI feedback mechanism but practical implementations in our scenario are feasible [16]. Nodes prefix each frame with a preamble to achieve time synchronization. Moreover, we use pilot symbols to estimate and correct CFO (Carrier Frequency Offset). At the physical layer, we modulate random data using OFDM parametrized equivalent to 802.11g, that is, 20 MHz channels, 54 usable subcarriers, 312.5 KHz subcarrier spacing, and 12.5% cyclic prefix. We assume  $n = 1$  and that  $N_P = 3$  subcarriers form a precoding block applying the subcarrier allocation as in Section II.

**Results.** Figure 4(a) shows our results for different modulation schemes. As expected, the BER degrades with higher orders of modulation. We also observe that OPV2-LD barely provides any improvement compared to ZF, while our approach OPV1-ONPM-ZF is significantly better. The reason is that LD poses a number of practical challenges. For instance, gains at the receivers must be set carefully to ensure that lattices fall on the expected locations. Moreover, time and frequency synchronization play a fundamental role. Investigating the effect of imperfect time synchronization in simulations, we found that LD suffers significantly from slight variations in frame detection. Regarding frequency synchronization, Figure 4(b) depicts the BER of OPV2-LD with estimated and ideal CFO as measured in our testbed. The results for ZF are shown for reference. While ideal CFO reduces the BER of ZF to half its value, for OPV2-LD it reduces the BER to less than a fifth, showing the impact of CFO on LD, i.e., LD requires a very accurate time and frequency synchronization at the receiver to perform well. In comparison, OPV1-ONPM-ZF is much less affected by real-world effects. Additionally, the complexity of OPV1-ONPM-ZF is only a fraction of the effort required for LD. Hence, OPV1-ONPM-ZF is better suited in practice than LD.

## V. CONCLUSIONS

In this work, we presented a new precoding vector optimization to improve the BER performance of the interference alignment scheme of [1]. Furthermore, we showed that our approach can be combined with other performance enhancement techniques for interference alignment such as orthonormalizing the precoding matrices and using lattice decoding instead of ZF to further improve the BER. Moreover, we

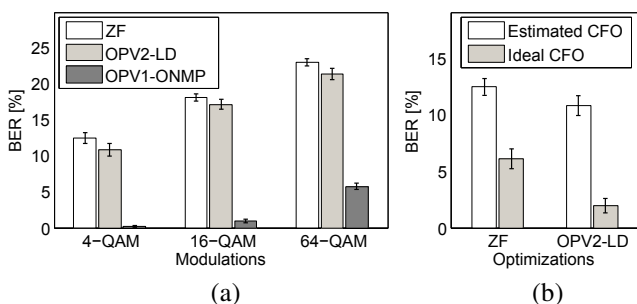


Fig. 4. BER measurements: (a) Increasing order of modulation with estimated CFO, (b) 4-QAM ZF and OPV2-LD with estimated vs. ideal CFO. Error bars indicate the 95 % confidence intervals over 100 experiment runs.

implemented interference alignment in the frequency domain along with the presented BER enhancement techniques on an SDR platform. Simulation results showed significant BER improvements for different  $M$ -QAM schemes compared to the original IA scheme of [1]. Testbed measurements revealed that our proposed precoding optimization in combination with ZF outperforms lattice decoding in practical systems due to its lower sensitivity to real-world effects, thus enabling IA also in lower SNR ranges.

## ACKNOWLEDGMENT

This work was performed within the LOEWE Priority Program Cocoon and the Collaborative Research Centre MAKI (SFB 1053) of the Deutsche Forschungsgemeinschaft (DFG).

## REFERENCES

- [1] V. R. Cadambe and S. A. Jafar, "Interference alignment and degrees of freedom of the k-user interference channel," *IEEE Trans. on Information Theory*, vol. 54, no. 8, 2008.
- [2] M. Shen, A. Host-Madsen, and J. Vidal, "An improved interference alignment scheme for frequency selective channels," in *Proc. IEEE International Symp. Inf. Theory*, 2008.
- [3] D. Kim and M. Torlak, "Optimization of interference alignment beamforming vectors," *IEEE Journal on Selected Areas in Communications*, vol. 28, no. 9, pp. 1425–1434, Dec. 2010.
- [4] P. Razaghi and G. Caire, "Interference alignment, carrier pairing, and lattice decoding," in *Proc. IEEE International Symposium on Wireless Communication Systems*, 2011.
- [5] O. Elayach, S. W. Peters, and R. W. H. Jr., "The practical challenges of interference alignment," *IEEE Wireless Communications*, pp. 35–42, Feb. 2013.
- [6] D. R. O. Gonzalez, I. Santamaria, J. A. Garcia-Naya, and L. Castedo, "Experimental validation of interference alignment techniques using a multiuser MIMO testbed," in *Proc. Workshop on Smart Antennas*, 2011.
- [7] J. Massey, J. Starr, S. Lee, D. Lee, A. Gerstlauer, and R. H. Jr., "Implementation of a real-time wireless interference alignment network," in *Proc. Asilomar Conference on Signals, Systems and Computers (ASCSSC)*, 2012.
- [8] V. R. Cadambe and S. A. Jafar, "Interference alignment and spatial degrees of freedom for the k user interference channel," in *Proc. IEEE International Conference on Communications (ICC 2008)*, May 2008.
- [9] S. Peters and R. Heath, "Interference alignment via alternating minimization," in *Proc. IEEE International Conf. Acoustics, Speech Signal Processing*, 2009.
- [10] K. Miller, A. Sanne, K. Srinivasan, and S. Vishwanath, "Enabling real-time interference alignment: Promises and challenges," in *Proc. ACM International Symposium on Mobile Ad Hoc Networking and Computing (MobiHoc)*, 2012.
- [11] H. V. Balan, R. Rogalin, A. Michaloliakos, K. Psounis, and G. Caire, "Achieving high data rates in a distributed MIMO system," in *Proc. MobiCom*, 2012.
- [12] T. Gou, C. Wang, and S. Jafar, "Aiming perfectly in the dark-blind interference alignment through staggered antenna switching," in *Proc. IEEE Global Telecommunications Conference (GLOBECOM)*, 2010.
- [13] A. Loch, T. Nitsche, A. Kuehne, M. Hollick, J. Widmer, and A. Klein, "Practical interference alignment in the frequency domain for OFDM-based wireless access networks," in *Proc. Symposium on a World of Wireless, Mobile and Multimedia Networks (WoWMoM'14)*, 2014.
- [14] M. O. Damen, H. E. Gamal, and G. Caire, "On maximum-likelihood detection and the search for the closest lattice point," *IEEE Trans. Inf. Theory*, vol. 49, no. 10, pp. 2389–2402, Oct. 2003.
- [15] "Rice Univ. WARP Project." [Online]. Available: <http://warp.rice.edu>
- [16] A. Loch, T. Nitsche, A. Kuehne, M. Hollick, J. Widmer, and A. Klein, "Practical challenges of IA in frequency," TU Darmstadt, SEEMOO, Tech. Rep., 2013. [Online]. Available: <http://www.seemoo.de/ia>